

# Design and fabrication of infrared detector arrays for satellite attitude control

A.W. van Herwaarden<sup>a,\*</sup>, F.G. van Herwaarden<sup>a</sup>, S.A. Molenaar<sup>a</sup>, E.J.G. Goudena<sup>b,1</sup>,  
M. Laros<sup>b,1</sup>, P.M. Sarro<sup>b,1</sup>, C.A. Schot<sup>b,1</sup>, W. van der Vlist<sup>b,1</sup>, L. Blarre<sup>c,2</sup>, J.P. Krebs<sup>c,2</sup>

<sup>a</sup> *Xensor Integration, Kanaalweg 1, 2628 EB Delft, Netherlands*

<sup>b</sup> *Dimes, Tu Delft, Feldmannweg 17, 2628 CT Delft, Netherlands*

<sup>c</sup> *Sodern, 20 av. Descartes, 94451 Limeil-Brevannes, France*

Received 8 August 1999; received in revised form 9 December 1999; accepted 21 December 1999

## Abstract

This paper describes the design, modelling and fabrication of infrared detectors for attitude control systems (ACS) for satellites. After a short introduction on the use and control of satellites in general, we explain the advantages of our integrated arrays of infrared detector units (pixels). Two types of detectors have been manufactured, a staggered array (ISA) with 32 pixels (in two staggered arrays of 16 pixels each) or in a cross of four staggered arrays (FPA) having 128 pixels in total. The choice depends upon the specific application (geostationary or GEO orbit or low-altitude orbit). The detectors are based on a bipolar silicon process for the mechanical structure (electrochemically controlled etching (ECE)-KOH etching), with a SiN membrane for thermal isolation of the pixels, which have a polymer black coating for transduction of radiation to heat and n-type vs. p-type polysilicon thermopiles for heat detection. The pixel pitch is 600  $\mu\text{m}$ , the black area is about  $495 \times 440 \mu\text{m}$  and the pixel sensitivity is about 55 V/W, at a thermopile resistance of 23.5 k $\Omega$ . The ISA measures in its present form  $13.5 \times 4 \text{ mm}$ , the FPA measures  $20.5 \times 20.5 \text{ mm}$ . © 2000 Elsevier Science S.A. All rights reserved.

*Keywords:* Infrared detector; Infrared array; Satellite

## 1. Introduction

Presently, we can see an increasing use of satellites orbiting around the earth for many applications. Originally used for espionage purposes, and later also for weather surveillance and communication, many dozens of satellites working in team effort are now responsible for highly accurate positioning systems (GPS), mobile-phone systems (satellite-constellations), and the whole communication and TV satellites in geostationary orbit. These satellites in an earth-bound orbit need attitude control systems (ACS) for a correct orientation of the platform with respect to the

earth. In this manner, antennas may be properly oriented with respect to relay stations on earth, or cameras will monitor the desired portion of earth's surface.

The increased use of such satellites and the ACS that come along is an incentive to develop new, cost-efficient instruments. The cost-efficiency is found not only in cheaper parts and assembly of the instrument, but also in better functionality and lower mass and size.

## 2. Attitude control of satellite platforms

The attitude control of a spacecraft is currently achieved by means of sensors which detect and measure the instantaneous directions of fields emitted by the surrounding celestial bodies: magnetic field, gravity gradient and optical radiation. Every time a sharp angular accuracy is required it is necessary to use optical radiation. Two types

\* Corresponding author. Tel.: +31-15-257-8040; fax: +31-15-257-8050.

*E-mail addresses:* svh@xensor.nl www.xensor.nl (A.W. van Herwaarden), sarro@dimes.tudelft.nl (P.M. Sarro), sodern@francenet.fr (L. Blarre), sodern@francenet.fr (J.P. Krebs).

<sup>1</sup> Tel.: +31-15-278-7708; fax: +31-15-278-7369.

<sup>2</sup> Tel.: +33-1-4595-7134; fax: +33-1-4595-7178.

of optical sensors are mainly used for the accurate stabilization of the platform of an Earth-orbiting satellite with respect to the Earth: Star Tracker and Earth Sensor [1,2]. The Star Tracker is an optical camera which images a star pattern on the focal plane of a CCD matrix array, and which can very accurately determine the orientation of the satellite in a Galilean reference coordinate system. The Earth Sensor is a thermal device which determines the edges of the infrared Earth in the 14–16  $\mu\text{m}$  wavelength band, and by doing this keeps the Sensor (and thus the platform) exactly oriented towards the Earth (centered or biased) with respect to the orbital reference coordinate system.

The Earth Sensor is generally less accurate than a Star Tracker, but more tolerant to space radiation and also much less costly. So it is very widely used for various types of ACS, especially for geostationary platforms where the required lifetime is the longest.

### 2.1. Earth Sensor based on infrared detector arrays

Present models of Earth Sensors are based on a single-element infrared detector which scans the Earth thanks to a rotating or oscillating mirror [1]. The mirror makes the detector scan a trace on Earth, so that it first crosses the Space–Earth transition in the North–West, and then the Earth–Space transition in the North–East (see Fig. 1). These transitions are measured by the detector in the 14–16  $\mu\text{m}$  band, in which Earth has a much higher emission than Space and which is not affected by day–night and season variations. The same then happens for the southern hemisphere. The exact location (in the reference frame of the Earth Sensor) is determined by comparing the transition moments with the mirror position timing.

Sodern in France (a subsidiary of Aerospatiale-Matra), a renowned manufacturer of both Star Trackers and Earth Sensors, wanted to develop a new generation of Earth

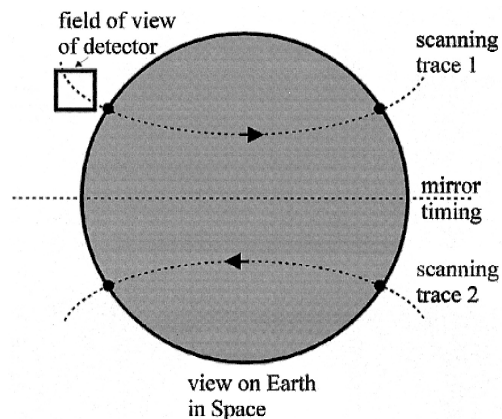


Fig. 1. In the single-element detector Earth Sensor, a rotating mirror projects a trace of Earth on the detector, enabling it to determine the Space–Earth transitions with respect to the Earth Sensor.

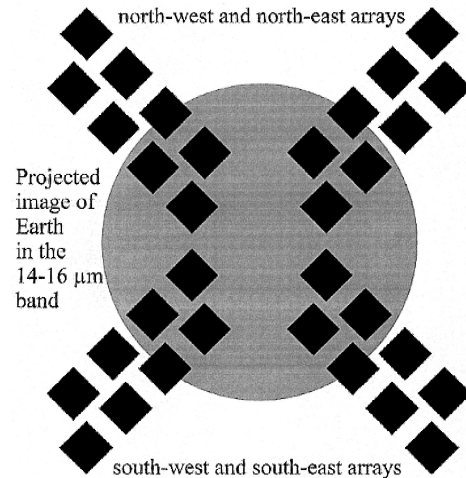


Fig. 2. In the Static Earth Sensor STS02 four infrared detector arrays of 32 pixels each (shown schematically) view the image of the Earth and determine its exact orientation with respect to the Static Earth Sensor, without using moving parts.

Sensors without moving parts. This leads to the Static Earth Sensor, which is more compact, smaller, lighter and more economic than Earth Sensors which use rotating or oscillating mirrors [1–3]. In addition, it also presents advantages in terms of longer lifetime, higher reliability and better instrument autonomy.

The basic idea of the new generation of Static Earth Sensors is to replace the single detector plus rotating mirror by four static arrays of infrared detectors. They continuously look at the northwest, northeast, southwest and southeast edges of Earth, thus removing the need for scanning. With arrays of 32 elements each, a good resolution of the Space–Earth transition can be obtained while maintaining a wide field of view, necessary to acquire Earth during launch or any other transfer orbit type. The configuration of the Static Earth Sensor then becomes as in Fig. 2.

Each array consists of 32 pixels (elements) which are arranged in two staggered arrays of 16 pixels next to each other. Staggered means that the arrays are shifted half a pixel length with respect to each other, and the effect of this is that there is always one pixel which has a full view of the Space–Earth transition. These arrays are called In-line Staggered Array (ISA), and Fig. 3 shows a photograph of the ISA together with multiplexer electronics.

For satellites in low or medium earth orbit (LEO or MEO orbit), the edges of Earth are on four opposite sides of the Earth Sensor instrument because the satellite is flying so low over Earth. In Earth Sensors for LEO and MEO applications, four separate germanium lenses are used to project the infrared image of the edges onto four separate arrays, and four ISA arrays are used in the instrument.

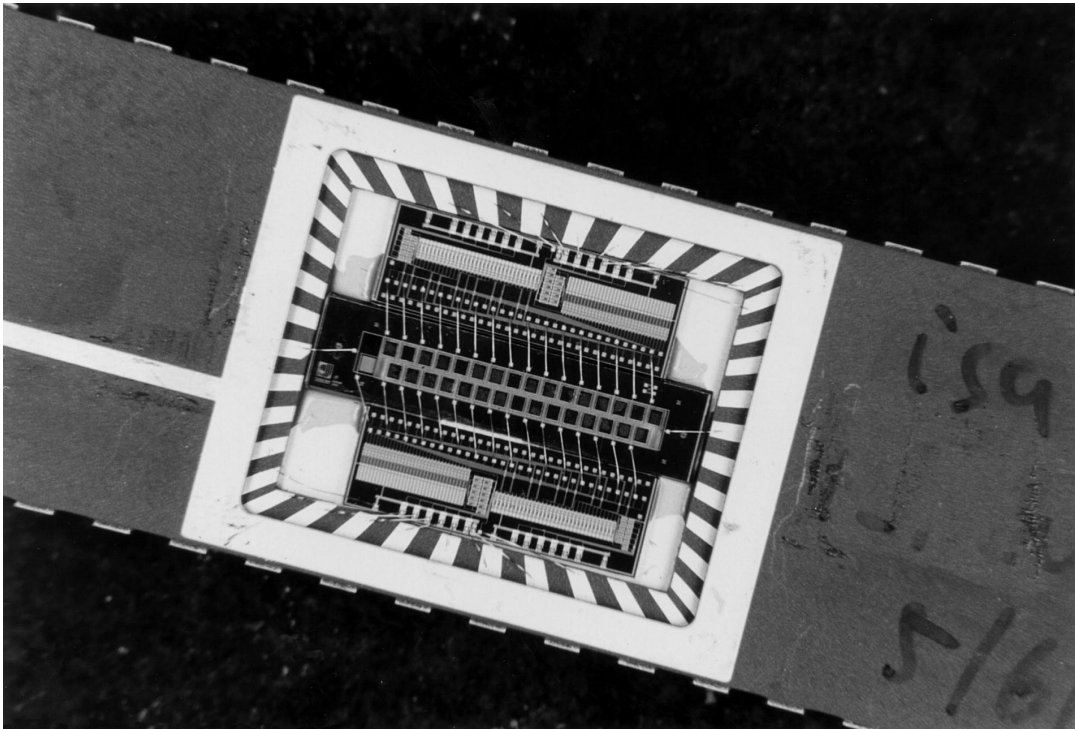


Fig. 3. Photograph of the ISA silicon infrared chip (size  $13.5 \times 4$  mm) containing a  $2 \times 16$  staggered array of infrared pixels to detect the edge of Earth in the  $14\text{--}16 \mu\text{m}$  band, with two CMOS radiation-hard multiplexers.

For a satellite in a geostationary orbit (GEO), the infrared image of the entire Earth is projected onto the detector by means of one single lens. In order to maximize

the dynamic range of the Earth Sensor (i.e., the ratio between highest and lowest altitude of the satellite where the Earth Sensor can still view the edge of Earth), it is

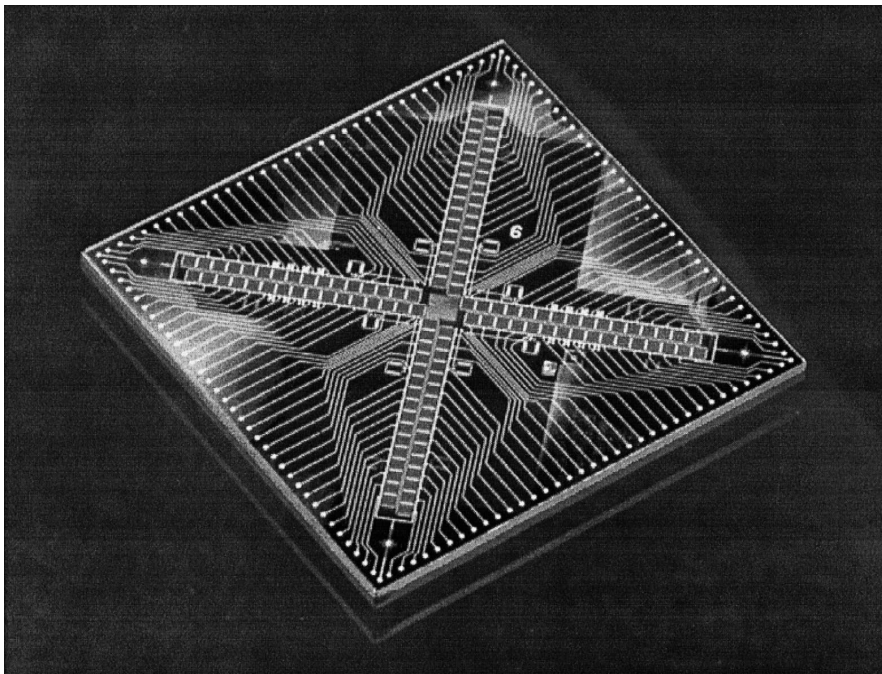


Fig. 4. Photograph of a FPA silicon infrared detector chip (size  $20.5 \times 20.5$  mm) integrating four ISA arrays for GEO applications.



Fig. 5. Photograph of the Static Earth Sensor STS02 for geostationary applications incorporating the FPA detector chip.

necessary to minimize the blind area in the center of the four detectors. By integrating the four ISA arrays in one chip, the blind spot in the middle can be reduced further than by using four separate array chips. This led to the design and fabrication of the Focal Plane Array (FPA) detector [4] (see Fig. 4).

This chip has a dynamic range of about  $10 \times$ , allowing operation from 15 000 up to 140 000 km altitude. Such an operating range is required because of the varying altitude of the satellite during the transfer orbit. The Static Earth Sensor brings a reduction in size, weight and power consumption of a factor of 2–3, compared to the present-day rotating-mirror Earth Sensor. This is also due to the very compact size of the FPA chip, which enabled Sodern to scale-down the entire design of the Earth Sensor. Fig. 5 shows the entire Static Earth Sensor, which is about  $13 \times 14 \times 15$  cm large. In Fig. 5, the bottom part is occupied by three layers of electronics, the analog electronics on top (closest to the detector, which is in the heart of the instrument). Below come the digital electronics, and at the bottom the power and communication electronics. Each board has connectors to the outside. Above the detector unit, the housing of the germanium lens can be seen, which is shaped to ward off stray radiation. Because the Earth Sensor will detect the Earth with an accuracy of less than  $0.1^\circ$ , a high degree of mechanical stability and proper mounting possibilities are required, and therefore a special housing has been developed for the entire instrument.

### 3. Modelling of pixels and arrays

Below, we will elucidate the fabrication and also modelling and design of the basic pixel, the ISA and the FPA. Fabrication is listed first, since the modelling and design is based on the fabrication technology at hand, which determines the material parameters and design possibilities of the devices to be modelled. Staggered arrays of infrared detectors have been fabricated before, e.g., Baer et al. [5]. They achieved a high pixel density with a high sensitivity by bulk etching of a long membrane accommodating all pixels. A low cross-talk was attained with silicon separation beams between the individual pixels. Other devices use front micromachining with arrays or matrices of bolometers, which can also be very sensitive in vacuum applications. However, we deal with ultralow signals (tens of  $\mu\text{V}$  only). A detector based on thermopiles with their inherent offsetless character is more convenient when going from a single element to 128 elements, than bolometers with their high offset and obligatory biasing circuitry, which also require thermal regulation and periodic calibration. Therefore, the choice of sensing element fell upon a thermopile-based sensor.

#### 3.1. Technology

At the University of Michigan, Baer et al. [5] obtained the silicon separation beams by a high p-type dose deposition ( $5 \times 10^{19} \text{ cm}^{-3}$ ), which prevents the silicon from being etched during micromachining [5]. At DIMES, we use a silicon–silicon nitride technology [6], in which n-type epilayer beams in a p-type environment are preserved using electrochemically controlled etching (ECE) in KOH [6]. Fig. 6 shows one of these beams as it has been etched out from the silicon substrate, the silicon-nitride membrane

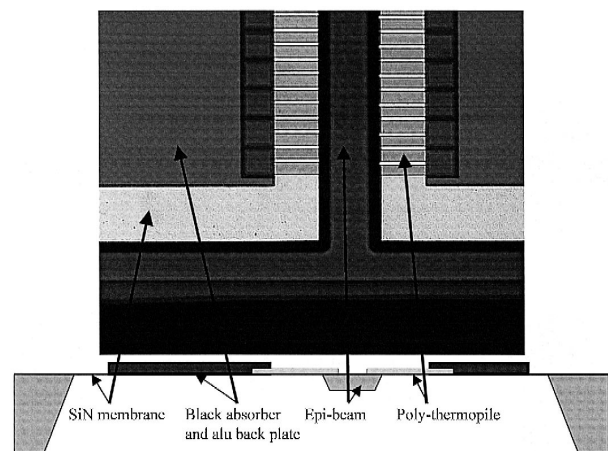


Fig. 6. Photograph from the back side of the chip. Details visible are the silicon beam etched out from the substrate for thermal isolation between infrared pixels, the aluminum back plates for temperature equalization, and the polysilicon thermocouples.

visible underneath. Visible to the left and the right of the silicon beam are polysilicon thermocouples and the absorbing areas of two neighboring pixels of the array (the aluminum back plate for temperature equalization, and some thin black lines showing the black absorber where the aluminum is left out).

The process we thus chose consisted of a standard bipolar or CMOS part, with lay-out measures and technology additions to enable ECE-KOH etching. The lay-out details include aluminum interconnection between the separate die in the sawing lane, with contacts openings to the epi-layer (locally doped for proper contact), and an aluminum contact area of typically  $1 \text{ cm}^2$  for electrical contact to the gold spring-loaded contact of the etching holder. Another measure is the removal of aluminum on the wafer edge. The bipolar/CMOS steps are used to create a mechanical structure, a thin-film add-on module is used to fabricate the silicon-nitride (low-stress) membrane and the p-type vs. n-type polysilicon thermopiles [7]. The process closely resembles that described in Ref. [6], with the addition of a second metal layer because of the complexity of the interconnection. An in-house black layer process is used to blacken the pixels and make them sensitive to infrared radiation in the 14–16  $\mu\text{m}$  band.

### 3.2. Modelling

We have modelled the required pixel and some possible array configurations in two manners, to obtain results for different parameters, and also to cross-check the validity of our modelling. On the one hand, we have used a simple discrete-element model allowing us to get an idea of sensitivity and time constant, and we used an EXCEL sheet to perform these calculations. We have also used ANSYS 5.3 for a FEM modelling, to arrive at the optimum configuration for the pixel design for parameters such as sensitivity and cross-talk. For this, we set up a 2-D model, since the detectors will be operated in vacuum, and no heat losses through air are present, and radiation losses can be neglected. A purely square-mesh model was used, each pixel was divided into squares of  $15 \times 15$  or  $25 \times 25 \mu\text{m}$ , giving up to a few thousand mesh points. No auto-meshing was used, since we used ANSYS to calculate for us the exact temperature on the two sides of thermopiles, the hot and cold side. To do this, we meshed in such a way that the temperature was calculated on those points exactly. The size of the mesh depended on the size of the thermopile, which was generally taken to be 30 or 50  $\mu\text{m}$  long. The width of the thermopile is of the order of 500  $\mu\text{m}$ . In the modelling we used the following thermal conductivity values (low-stress SiN  $\approx 3 \text{ W/Km}$ , mono-Si  $\approx 150$ , poly-Si  $\approx 30$ , aluminum  $\approx 200$ , oxide  $\approx 1.5$ ), and a Seebeck coefficient of 230  $\mu\text{V/K}$  for the polysilicon. The ANSYS modelling has been based on a six-pixel part of the array, one pixel being irradiated by Earth, the other

five not. In this way, we have established the sensitivity of an irradiated pixel, by dividing the calculated temperature difference vs. input radiation power, and we have determined the cross-talk. In particular, Sodern wanted to optimize the Quality Factor for the pixels [8], given by the formula:

$$QF = AS / (\sigma_d^2 + \sigma_e^2)^{0.5}$$

where  $A$  is the active area of the pixel in  $\text{m}^2$  (prescribed by Sodern),  $S$  is the pixel sensitivity in  $\text{V/W}$ ,  $\sigma_d^2$  is the square of the detector noise ( $\approx 4 \text{ kTR}$ ) and  $\sigma_e^2$  is the same for the electronics,  $\sigma_e < 20 \text{ nV}/\sqrt{\text{Hz}}$ . The QF was eventually optimized to above  $500 \text{ m}^2 \text{ Hz}^{1/2} \text{ W}^{-1}$ . For this optimisation, we have varied the size of the silicon-nitride membrane, varied the sizes of the silicon beams used to thermally separate the pixels, and varied the thermopile length (typically 30–50  $\mu\text{m}$ ) and the black absorber area. But this area was mainly determined by the specifications of Sodern. The value of QF has been calculated both with EXCEL models (based on discrete element, each pixels being composed of a capacitance and two or three thermal resistances) and with the ANSYS model.

Fig. 7 shows an example of the graphical output from EXCEL, numerical output has been acquired as well. Fig. 7 clearly shows the improvement in the temperature homogeneity that is accomplished by using an aluminum back plate underneath the black area. The design targets and the values measured on manufactured devices are given in Table 1. Only the electrical resistance is slightly higher

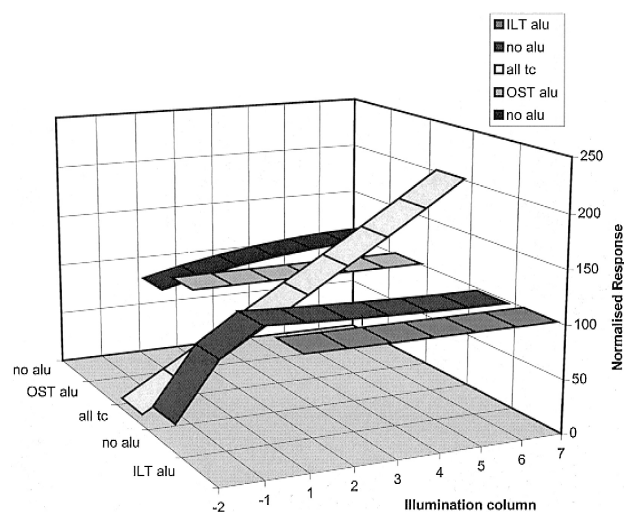


Fig. 7. Graphical output of EXCEL on the modelling of a pixel for various configurations with or without aluminium back plate, showing the improvement in temperature homogeneity due to the aluminium back plate. Shown is the response of the sensor for illumination in anyone of the seven columns of 25  $\mu\text{m}$  width. The OST (structure with thermopiles perpendicular to the array axis) and the ILT (structure with the thermopile in line with the array axis, as in the ISA and FPA devices fabricated later on) give similar results on temperature homogeneity, without aluminium back plate, there is some inhomogeneity in response.

Table 1  
Main characteristics of ISA/FPA chip

Parameter	Design value	Experimental value	Unit
Chip size ISA	as small as possible	13.5 × 40.0	mm
Chip size FPA		20.5 × 20.5	
Pixel pitch	600	600	μm
Active area	495 × 440	495 × 440	μm
Poly-silicon thickness		300	nm
P-type poly sheet resist		75	Ω/sq
N-type poly sheet resist		50	Ω/sq
Pixel resistance	< 15	23.5	kΩ
Temperature coefficient of resistance		−0.1	%/K
Uniformity of resistance		< 4	%
Sensitivity (in vacuum)	> 50	55	V/W
Temperature coefficient of sensitivity	< 0.25	+0.2	%/K
Uniformity of sensitivity	< 10	< 10	%
Time constant	< 16	< 10	ms
Radiation tolerance	100	> 400	krad

than originally intended, but in combination with the electronics processing the detector signals, this turned out to be permissible.

## 4. Fabrication

### 4.1. Redesign considerations

The modelling led to a few different alternatives which were then fabricated and measured [4]. In particular, we tried two different designs with a single array of 32 pixels and one with two staggered arrays of 16 pixels (called ISA). The single arrays have the disadvantage of blind areas, but the design with staggered arrays does not have this disadvantage, and was chosen for the subsequent developments. These were fabricated in the standard DIMES CMOS process with the addition of the thin-film thermopiles and the ECE-KOH provisions. The batch also included CMOS multiplexers with a design that was made radiation hard by surrounding all transistor gates by guard rings and making a spacious design (see Fig. 2).

The ISA detectors made in the first batch showed that some minor process adjustments were needed to arrive at the proper geometry and electrical resistance of the pixels. This was done in the second batch, which yielded satisfactory ISA arrays. The multiplexers fabricated in the first batch performed as designed. They successfully withstood several hundred kRad of radiation, demonstrating their radiation hardness in space. However, Sodern wanted to go into the direction of the FPA concept, with four ISA detectors on one chip. The size of this FPA design, which was eventually squeezed into 20.5 × 20.5 mm, required a complicated lithographic processing. Therefore, the concept of combining the FPA and multiplexers on a single chip was abandoned. Instead, the FPA chip is mounted in a ceramic hybrid with the multiplexers around it (see Fig. 8), in a special metal ring for suspension in the Earth Sensor instrument.

### 4.2. Mixed stepper and contact masks

Because of the large area of the FPA chip, and the necessity to treat the wafer edge for the ECE-KOH etching, a complicated lithographic processing is necessary. The detector design requires a typical alignment accuracy of 1 μm. Considering the typical thermopile length of only 30–50 μm, the submicron alignment accuracy of the wafer stepper is much preferred over the 5 μm alignment accuracy of the manual contact aligner at DIMES. And because of the very high number of contact openings and polysilicon thermocouples (per device of the order of 20000 contact openings and about 5000 thermocouples), a contactless lithography is preferable for yield. On the other hand, the overall FPA chip design is 29 × 29 mm, when measured orthogonally, too large for the wafer stepper (ASM 2500) which will expose areas of 10 × 10 mm maximum. Therefore, we combined stepper masks and contact masks. In total, seven full-wafer contact masks and two sets of 10 stepper masks have been used, with one set of stepper masks for the horizontal arrays and one set for the vertical arrays. In total, 24 masks have been used to fabricate the chips which is made in 14 mask steps. Three mask steps are performed using both stepper and contact masks, seven steps use only contact masks and four steps use only stepper masks. Because the stepper masks do not fill the entire area, those lithography steps which are used to remove layers rather than define windows (the first metal layer and the polysilicon layer) were defined in three masks, a horizontal and vertical stepper mask and a contact mask. Also, the CO mask for contact openings to the epilayer and the polysilicon thermopiles was designed in mixed masks because the small thermopiles require very accurate alignment, while the openings to the epilayer (for the ECE-KOH etching) require large area covering. The second metal layer was not used for fine details, and could be made in a contact mask entirely. Next to eight FPA chips each wafer also contains four separate ISA arrays, which enables quick and easy testing of the array proper-

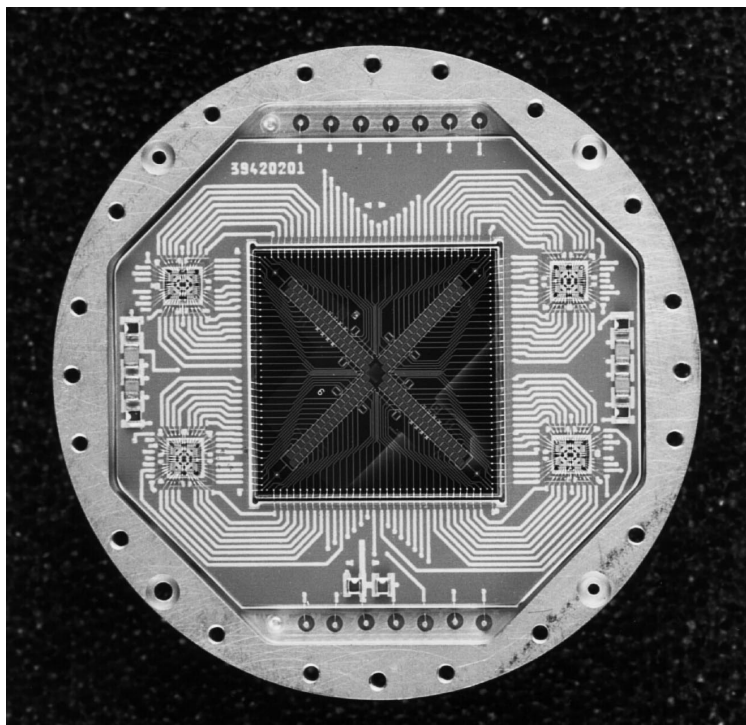


Fig. 8. The FPA detector chip mounted in a ceramic hybrid with radiation-resistant multiplexers inside a metal suspension ring.

ties. This is more convenient than mounting the FPA in its special hybrid, which is a time-consuming and costly affair.

## 5. Experimental results

Extensive measurements have been made on the ISA devices, including measurements of their radiation hard-

ness. As might be expected, radiation is not a problem for devices such as these, which electrically consist of active layers (polysilicon and aluminum) separated by dielectric layers (silicon dioxide and nitride).

The measured values for some characteristic parameters are listed in Table 1, together with the design targets. This shows that the chips fully function as originally intended, with the only compromise in a slightly higher pixel resis-

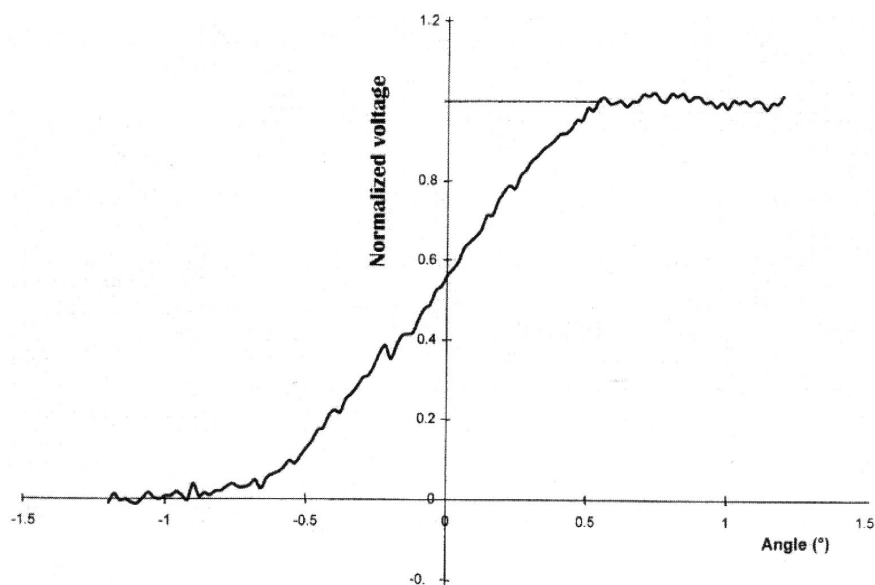


Fig. 9. Normalised angular response of one pixel.

tance. However, by keeping the spread in pixel resistance low, this is acceptable.

Fig. 9 shows the normalised output of a pixel when the Earth–Space transition is moving across the absorbing area. After compensation by software of distortions, a linearity error of less than  $0.025^\circ$  remains.

## 6. Conclusion

For the new generation of Earth Sensors, instruments for accurately aligning satellites with Earth, new infrared sensor arrays, both single ISA with 32 pixels and FPAs with four ISA-arrays in a cross, have been designed and fabricated. After initial modelling and fabrication of test designs, an optimized array was eventually designed and fabricated meeting all the major requirements and confirming the modelling results.

The chips, which integrate one (ISA) or four (FPA) infrared detector arrays on a single die, allow the fabrication of Earth Sensors without any moving parts, with a 2–3 fold reduction of size, weight (from 3.3 to 1.1 kg) and power consumption (from 7.5 to 3.5 W).

## References

- [1] O. Brunel, J.P. Krebs, Flight Results of a New GEO Infrared Earth Sensor STD 15 on Board TC2, AAS 93-324, pp. 1–15.
- [2] J.P. Krebs, L. Blarre, G. Coste, D. Vilaire, A new Family of low cost Attitude Control Sensors, 49th Int. Astronautical Congr. Melbourne Australia, Sept 28–Oct 2, 1998, IAF-98-U.5.06.
- [3] J.P. Krebs, R. Navoni, New Static Earth Sensor STS02 for GEO Platforms, Int. Workshop on Spacecraft Attitude and Orbit Control Systems, ESTEC, Noordwijk, the Netherlands, 15–17 Sept. 1997.
- [4] A.W. van Herwaarden, F.G. van Herwaarden, S.A. Molenaar, B. Goudena, M. Laros, P.M. Sarro, C.A. Schot, W. van der Vlist, L. Blarre, J.P. Krebs, Fabrication of a Focal Plane Array Infrared Detector for a Satellite Attitude Control System, Proc. Transducers '99, Sendai, Japan, June 7–10, 1999, 2D3.1.
- [5] W.G. Baer, K. Najafi, K.D. Wise, R.S. Toth, A 32-element micromachined thermal imager with on-chip multiplexing, Sens. Actuators, A 48 (1995) 47–54.
- [6] P.M. Sarro, A.W. van Herwaarden, W. van der Vlist, A silicon–silicon nitride fabrication process for smart thermal sensors, Sens. Actuators, A 42 (1994) 666–671.
- [7] P.M. Sarro, Sensor technology strategy in silicon, Sens. Actuators, A 31 (1992) 138–143.
- [8] J.P. Krebs, L. Blarre, D. Guillon, Low Cost Static Infrared Earth Sensors for Small and Micro-Satellites in LEO, 4th Int. Symp. Small Satellites Systems and Services, Antibes-Juan les Pins, Sept. 14–18, 1998.